Amino Acids (2009) 37:693–701
DOI 10.1007/s00726-008-0189-4

ORIGINAL ARTICLE

L-Leucinamide hydrogensquarate: spectroscopic and structural elucidation

Tsonko Kolev · Sonya Zareva · Heike Mayer-Figge · Michael Spiteller · William S. Sheldrick · Bojidarka B. Koleva

Received: 4 July 2008 / Accepted: 26 September 2008 / Published online: 25 October 2008

Abstract The hydrogensquarate [LeuNH$_2$] (HSq) of L-leucinamide has been synthesized and its structure has been determined by single crystal X-ray diffraction. A three dimensional network is formed by hydrogen bonds with participation of the O=C–NH$_2$ function, the hydrogensquarate ion and the N$^+$H$_3$ group [NH$_2$···O=C$_{(Sq)}$ (2.840 and 2.749 Å), $_{(Sq)}$OH···O=C(NH$_2$) (2.618 Å), NH$_3^+$···O=C$_{(Sq)}$ (3.246, 2.804 and 2.823 Å)], respectively. A theoretical approximation of the electronic structure was carried out by means of ab initio UMP2 and MP2 level of theory at the 6-311++G** basis set. The IR-spectroscopic assignment in the solid-phase was obtained by linear-polarized IR-spectroscopy of oriented samples as colloid suspensions in a nematic host and application of the reducing-difference procedure for the interpretation of polarized IR-spectra.

Keywords L-Leucinamide hydrogensquarate · Crystal structure · Solid-state IR-LD spectroscopy · ab initio calculations · ^{1}H-NMR data

Introduction

Intermolecular hydrogen bonds, characterized by low binding energies of typically 10–30 kJ mol^{-1} and allowing biomolecules to interact weakly with their targets before being released, are proposed as a basis of the biological activities of many molecules in biochemical processes. In vivo biochemical processes often involve a combination of intra- and intermolecular hydrogen bonding interactions, the details of which are not always well understood.

Amino acids are the simplest biomolecules to allow intramolecular hydrogen bonds, and serve as building blocks of the more complex peptides and proteins. Accurate structure determination and the identification of intramolecular hydrogen bonding motifs in these systems may provide an insight into the interactions in larger systems as well as rendering valuable experimental data for testing and refining ab initio methods. However, polypeptides in the living cell are joined together by amide linkages and the intramolecular hydrogen bonding networks in peptides are better represented by amino amides than amino acids. Therefore, amino acid amide derivatives may be viewed as simple peptide models.

Structural studies on some C-α-amidated amino acids Ile, Val, Thr, Ser, Met, Trp, Gln, Arg (In et al. 2001) and Tyr (Kolev et al. 2006a) have been performed and compared with their C-α-unamidated counterparts (In et al. 2001). It is known that the corresponding to most mammalian peptide hormones possess a C-α-terminal-amide as exemplified by calcitonin, gastrin, neurokinins,

Electronic supplementary material The online version of this article (doi:10.1007/s00726-008-0189-4) contains supplementary material, which is available to authorized users.

T. Kolev · M. Spiteller
Institut für Umweltforschung,
Universität Dortmund, Otto-Hahn-Strasse 6,
44221 Dortmund, Germany

S. Zareva
Faculty of Chemistry, University of Sofia
"St. Kl. Ohridsky", 1164 Sofia, Bulgaria

H. Mayer-Figge · W. S. Sheldrick · B. B. Koleva (✉)
Lehrstuhl für Analytische Chemie,
Ruhr-Universität Bochum,
Universitätsstraße 150, 44780 Bochum, Germany
e-mail: BKoleva@chem.uni-sofia.bg

neuropeptides and their related peptides (Eippe and Mains 1988). In many cases C-α-amides are much more biologically active in comparison to the corresponding C-α-terminal free acids. The importance of the C-α-terminal-amide for bioactivity can be illustrated by the "potency ratio", which is defined as the relative potency of a peptide amide divided by the relative potency of the corresponding peptide free acid, e.g. neurocinin A possesses potency ratio >10,000 (Merkler 1994; Suwan et al. 1994). At present, the biological structure-activity function of C-α-amides is not fully understood. The amidation arises from the oxidative cleavage of C-α-terminal glycine-extended prohormones (Kulathila et al. 1999). Since the protonated form of amino acid amides exists in the living cell, such information may be useful to understanding the different biological functions of C-α-amides and C-α-acid peptides.

On the other hand, the bioactive role not only of the neutral peptides but also of their protonated forms is also known to be connected to the different possible conformations of peptide chains. Moreover, most in vivo conditions are characterized by a weakly acid medium, resulting into protonated active forms of both peptides and proteins. The choice of the acidity agent for in vitro investigations is dependent on from its own bioactive function. Squaric acid (H_2Sq) is an alternative for studying the protonated forms and amides of amino acids and peptides. Its application for the synthesis of optically active derivatives of amino acids, with potential nonlinear optical and electro-optical properties is known (Kolev et al. 2007a, 2008a; Wolff and Wortmann 1999; Chemla and Zyss 1987; Nalwa et al. 1997). However, its important biorole has been intensively studied in last decade. A large number of medications based on H_2Sq derivatives are known (Sztaricskai et al. 2005; Tevyashova et al. 2004). Some amides of H_2Sq are effective monoanionic inhibitors of protein tyrosine phosphatases (Xie et al. 2004), other derivatives are selective inhibitors of DNA polymerases from several viruses (Xie et al. 2004). The H_2Sq amides of antracycline glycoside-type antibiotics such as daunomycin, adriamycin, epirubicin and carminomycin are potential antitumor agents as far as the corresponding nonsubstituted drugs are widely used in cancer chemotherapy (Kim and Misco 1992). In recent years the bioactivity of H_2Sq and some derivatives as inhibitors and VLA-4 integring antagonists (Nalwa et al. 1997) or potassium channel openers (Sztaricskai et al. 2005; Tevyashova et al. 2004) has also been reported. The systematic investigation of amino acid amides and their derivatives with H_2Sq and diethylsquarate is a requirement for understanding the properties and spectral assignments of di-, tri-, tetra- and polypeptides role. The mentioned model systems describe adequately the peptide properties and on the other hand are potential bioactive substances. During the last 2 years a series of structural studies on amino acid amides, including hydrogensquarates of alaninamide, prolinamide, tyrosinamide, argininamide and ester amides of squaric acid of phenylalaninamide, methioninamide, alaninamide, prolinamide, valinamide and triptophanamide have been carried out (Kolev et al. 2004, 2005, 2006a, b, c, d, e). In all cases, the influence of intra and intermolecular interactions on the vibrational spectra in the solid-phase has been characterized and some structural predictions have been made using the possibilities of the linear-polarized IR-spectroscopic approach of oriented solid-samples as suspensions in a nematic liquid crystal (Ivanova et al. 2004, 2006, 2007; Koleva et al. 2008).

For above reasons, the purpose of this work is to investigate the structure and IR-spectroscopic properties of L-leucinamide hydrogensquarate ($LeuNH_2{\cdot}HSq$) shown in Scheme 1 using the methods of single crystal X-ray diffraction and polarized infrared linear-dichroic (IR-LD) spectroscopy, based of an orientation technique of a solid guest sample as a colloid suspension in a nematic liquid crystal. The possibilities of this new approach for obtaining IR-spectroscopic and structural information have been demonstrated for series of peptide systems (Ivanova et al. 2004, 2006, 2007; Koleva et al. 2008). The assignment of characteristic IR bands of L-leucinamide hydrogensquarate has been performed by comparing experimental IR-spectroscopic and theoretical data with a view to explaining the changes in the condensed phase as a result of intermolecular interactions. The theoretical approximation of the electronic structure is presented as well using ab initio calciulations at the UMP2 and MP2 level of theory with a 6-311++G** basis set.

The usage of the H_2Sq as corresponding counter ion in the crystals of the amino acids and their derivatives is fruitful as far as for this compound has been observed a considerable progress in recent years by controlling the assembly of individual molecules in solids. By tunning the hydrogen bonding as a powerful non-covalent force for organizing organic molecules a series of derivatives of H_2Sq with small biologically active compound have been

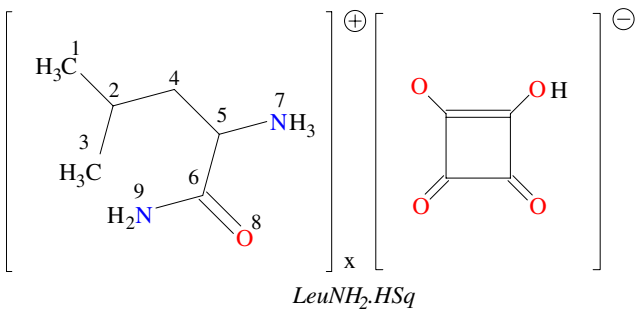

LeuNH2.HSq

Scheme 1 Chemical diagram of the compound studied

obtained (Ivanova et al. 2004, 2006, 2007; Koleva et al. 2008). H_2Sq provides an attractive template for generating tightly hydrogen bonded self-assemblies from polarizable cations in general and basic amino acids in particular. The self-assembly patterns of H_2Sq itself and its anions HSq^- and Sq^{2-} have been identified. It is reasonable to expect that a further systematic variation of the counterion in salts of the HSq^- and/or Sq^{2-} anions should lead to the isolation of additional different conformers of the amino acids and their derivatives, diving a possibility for direct elucidation of the relationship structure-spectroscopic properties of these systems.

Experimental

Synthesis

$LeuNH_2{\cdot}HSq$ was synthesized in the following way: a 3 ml ethanol solution of L-leucinamide (2 mmol, 0.3060 g) was mixed with solutions of 0.22 ml H_2Sq and 0.27 ml thriethylamine both in 2 ml ethanol. The obtained mixture was stirred for 3 h, after which the resulting white precipitate was filtered off and recrystalized from ethanol. After 2 weeks, colorless crystals were isolated and filtered and dried at room temperature. Found: C 49.20, H 6.60, N 11.48, $[C_{10}H_{16}N_2O_5]$ calculated: C 49.18, H 6.60, N 11.47%. The most intensive signal in the mass spectrum of the compound is the peak at *m/z* 131.31, corresponding to the singly charged cation $[C_6H_{15}N_2O]^+$ with a molecular weight of 131.20. TGV analysis in the range 350–500 K showed an absence of the solvent molecules in the unit cell of the compound. ^{1}H-NMR spectra of the compound are shown in Fig. 5 and are characterized by the chemical shifts of the leucine α_{CH}, β_{CH2}, γ_{CH} and δ_{CH3} protons at 0.990, 1.719, 3.298, 3.908.

Methods

The X-ray diffraction intensities were measured on a Siemens P4 diffractometer equipped with MoK_α radiation ($\lambda = 0.71073$ Å). The structure was solved by direct methods (Sheldrick 1997a) and refined against F^2 (Sheldrick 1997b). An ORTEP plot illustrates the structure at the 50% probability level (Fig. 1). Relevant crystal data and refinement details are presented in Table 1, selected bond distances and angles in Table S1 (supporting materials). The hydrogen atoms were positioned at calculated sites.

The 4,000–400 cm^{-1} solid-state IR-spectra were recorded on Bomem Michelson 100 FT-IR Spectrometer (resolution 2 cm^{-1}) equipped with a Perkin-Elmer wire-grid polarizer. The conventional (non-polarized) solid IR-spectra are scanned using standard procedures as Nujol mull and KBr pellets. The oriented solid-samples are obtained by the orientation technique as a suspension in NLC using of 4-cyano-4′-alkylbicyclohexyl type (ZLI 1695, Merck) mixture (Scheme 2). The following reasons enforced its choice: (1) its poor IR-spectrum allows recording the guest-compound bands in the whole 4,000–400 cm^{-1} range. The presence of an isolated nitrile stretching IR-band (ν_{CN}) at 2,235 cm^{-1} additionally serves as an orientation indicator; (2) the mesomorphic interval included the room temperature; (3) the low dielectric constant of 4.2 ($\varepsilon_\parallel = 7.8$ and $\varepsilon_\perp = 3.6$ at 20°C) is an

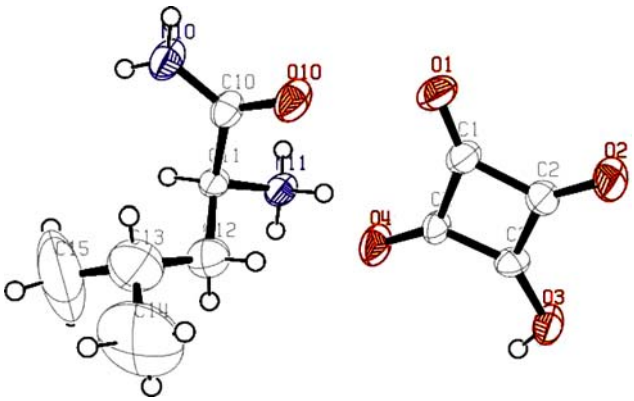

Fig. 1 ORTEP plot of the asymmetric unit of $LeuNH_2{\cdot}HSq$ at 50% probably thermal ellipsoids

Table 1 Crystal data, data collection and refinement conditions

Empirical formula	$C_6H_{15}N_2O$, C_4HO_4
Formula weight	244.25
Temperature	294(2) K
Wavelength	0.71073 Å
Crystal system, space group	Orthorhombic, P 2(1)2(1)2(1)
Unit cell dimensions	$a = 7.4690(15)$ Å $\alpha = \beta = \gamma = 90.0°$
	$b = 8.3006(17)$ Å
	$c = 21.838(4)$ Å
Volume	1353.9(5) $Å^3$
Z	4
Calculated density	1.198 Mg m^{-3}
Absorption coefficient	0.097 mm^{-1}
F(000)	520
Crystal size	0.59 × 0.40 × 0.28 mm
2θ range for data collection	$2\theta < 50°$
Limiting indices	$0 \le h \le 8$, $0 \le k \le 9$, $-25 \le l \le 25$
Absorption correction	Semi-empirical
Refinement method	Full-matrix least-squares on F^2
Reflections collected/unique	2,373/1,133 [R(int) = 0.0159]
Data/restraints/parameters	1,133/3/157
Goodness-of-fit on F^2	0.936
Final R indices [$I > 2\sigma$ (I)]	$R_1 = 0.0719$, $wR_2 = 0.1333$
R indices (all data)	$R_1 = 0.1819$, $wR_2 = 0.1616$

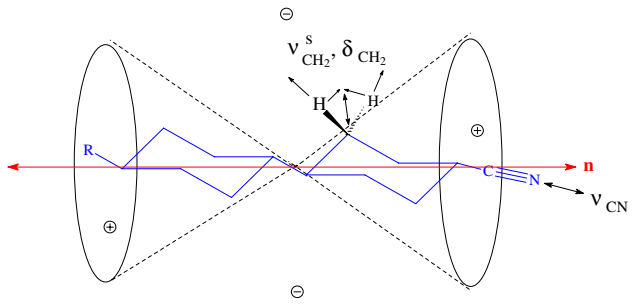

Scheme 2 Chemical diagram of the nematic host

important parameter of IR-spectral materials; (4) clearing point 72°C, viscosity at 20°C is 62 mm^2/s and the optical anisotropy at 20°C and 589 nm is $\Delta n = 0.06$, $n_e = 1.531$ and $n_o = 1.468$, respectively. The effective orientation of samples is achieved by means of the following procedure: 5 ± 1 wt % of the compound studied is mixed with the NLC until a slightly viscous suspension was obtained. Thus prepared phase is pressed between two KBr plates, previously rubbed out by means of fine sand-paper (C800) in one direction, coinciding with orientation one (**n**). The grinding of the mull in the rubbing direction promotes additional orientation of the sample. Each IR-LD spectrum is based on 150 scans at room temperature, 25°C. The determination of the position (ν_i) and their integral absorbances (A_i) are carried out by preliminary deconvolution and subsequent curve-fitting procedure at mixed Lorentzian to Gaussian peak functions at ratio 50:50%, the χ^2 factor varied within 0.0004_7–0.0003_9.

The difference-reducing procedure for linear-polarized IR-spectra interpretation consists in subtraction of the perpendicular spectrum (IR_s), resulting from 90° angle between the polarized light beam electric vector and the orientation of the sample from the parallel one (IR_p), obtained with a co-linear mutual orientation. The recorded difference ($IR_p - IR_s$) spectrum divides the corresponding parallel (A_p) and perpendicular (A_s) integrated absorbances of each band into positives, originating from transition moments which form an average angles with the orientation direction (**n**) between 0° and 54.7° (magic angle) and the negative ones, corresponding to transition moments between 54.7° and 90°. In the reducing-difference procedure, the perpendicular spectrum multiplied by the parameter ***c***, is subtracted from the parallel one and ***c*** has to be varied until one selected band or set of bands are eliminated. The simultaneous disappearance of these bands in the obtained reduced IR-LD spectrum ($IR_p - \boldsymbol{c}IR_s$) indicates a co-linearity of the corresponding transition moments, yielding information about the mutual disposition of the molecular fragments. This elimination method is graphically carried out using a subtracting procedure supplementing the program for processing of IR-spectra.

The presented determinations are results of the following equations, definite for i-band with ν^i ($i = 1,\ldots,n$): $(A_p^i - A_s^i) = A^{iso} \cdot S \cdot (3/2\cos^2\theta - 1/2)$, where S is so-called orientation factor, showing the average orientation of the molecule, and varies between 0 and 1 (Ichikawa and Iitaka 1969; Michl and Thulstrup 1986). If the $S = 0$, the effective orientation of the molecule is not observed, while at $S = 1$ maximal orientation exists. It is known that in the technique of orientation as nematic liquid crystal solution, S depends on geometry and size of the guest molecule, temperature and especially on the amount of the mesomorphic medium; A^{iso} is the integral absorption of the i-band in the corresponding non-polarized spectrum and θ is the angle between the i-transition moment towards the orientation direction (**n**).

If $\theta = 0$, then $(A_p^i - A_s^i) = A^i$, $(A_p^i - A_s^i) > 0$ and the corresponding peak is positive. To $\theta = 90°$ the $(A_p^i - A_s^i) = A^i S$, and $(A_p^i - A_s^i) = -1/2A^i S < 0$ lead to negatively oriented peak. If $\theta = 54.7°$, then $A_p^i = A_s^i$ and the peak is not observed in the difference IR-LD spectrum. These dependencies and conclusions could be illustrated using the polarized IR-LD spectra of ZLI 1695. A positive in the difference spectrum maximum at 2,235 cm^{-1} (ν_{CN}) arise because of the ν_{CN} transition moment closed an angle between 0° and 54.7° with (**n**). In contrast, the negative peak at 1,450 cm^{-1} corresponds to $\delta^s_{CH_2}$ with transition moments between 54.7° and 90° with (**n**) (Scheme 2).

The interpretation of IR-spectra with multiple or strongly overlapped peaks not only in polarized but also in conventional IR-spectrometry request as first step to determine the number of peaks and their subsequent c_{CN}urve-fitting resulting in ν_i and integral absorption A_i values. The deconvolution based on Fourier-Self Deconvolution method and the next peak-fitting procedure is applied in this respect.

The curve-fitting of peaks includes the Levenberg-Marquardt method, where the algorithm continually iterates until a minimum value of the reduced χ^2 is reached. The χ^2 is actually a statistical measure of the "goodness-of-fit", based on the known variance in the data. This approach is defined as curve-fitting or peak-fitting procedure. During the curve-fitting of the IR-spectral curve three peak functions should be chosen, a Lorentzian, Gaussian or mixed Gaussian and Lorentzian peak functions. The mixed Gaussian and Lorentzian peak function has proved the most useful in IR-spectral interpretation. The optimization of this procedure for the orientation of the solid-samples as well that used for IR-spectra interpretation have been described in (Ivanova et al. 2004, 2006, 2007; Koleva et al. 2008). The position (ν_i) and integral absorbancies (A_i) for each i-peak were determined by deconvolution and curve-fitting procedures at a 50:50% ratio of Lorentzian to Gaussian peak functions with χ^2 factors within

0.00047–0.00039 following 2,000 iterations. The means of two treatments were compared by use of a Student t test. The sand-papers with sizes C100–C800 are SIA (Switzerland) products.

All the IR-spectra interpretations are made on CRAMS AI/7 IR-spectroscopy (2001, Thermo Galactic, 395 Main Street, Salem, NH 03079 USA, WEB: http://thermogalactic.com) and Statistica 5.11 [StatSoft, Inc. (1998), 2300 East 14th Street, Tulsa, OK, 74104, USA; WEB: http://www.statsoft.com] program packages for statistic treatments.

The theoretical analysis was performed using the GAUSSIAN 98 (1998) program package. The conformational analysis of compound studied in gas phase was carried out in the follow way. To generate the (φ,χ) potential energy surface, the structures were calculated at the ab initio UHF/6–31G*//UHF/6-311++G** and RHF/6-31G*//RHF/6-311++G** levels. The geometry was then fully relaxed, except for the constrained torsion angles φ and χ. Values of these angles were chosen by using a step size of 0.5°, within the range from −180° to 180° (Head-Gordon et al. 1991). The minima observed on the surface were then subjected to full geometry optimization at the UMP2 and MP2 level with the l6-311++G** basis set, which should enable correct prediction of the stability order of the calculated minima (Vargas et al. 2002). This was then followed by a second-derivative analysis (frequency), which proved all of them to be minima. The absence of imaginary frequencies, as well as of negative eigenvalues of the second-derivative matrix, confirmed that the stationary points correspond to minima of the potential energy hypersurfaces. The geometrical parameters of the corresponding energy-minimized conformers were further discussed. The accessible conformational space of the molecule was assumed on the basis of the close resemblance between the Ramachandran contact map and the energy contours map within the limit of 5.0 kcal mol^{-1} (Ramachandran and Sasisekharan 1968), as is also applied elsewhere (Zimmerman et al. 1977) The space was calculated with the Surfer 8 program using the radial basis function as a girding method. As the overall conformational profiles of modified peptide models can differ from those of common peptide models, we describe the energy-minimized conformers of the investigated molecule by the general short hand letter notation introduced by (Zimmerman et al. 1977). The minimization of energy takes place by optimization of dihedral angles and Table 1 contains the data for the most stable conformers. The torsion angle φ is determined by the relative disposition of the cationic NH and electronegative carbonyl atoms. χ_1 is defined as $N(NH)_i$–C_j–C_k–C_l, for the conformation in the amino acid amide side chain. For a comparison the most stable conformer of the compound studied is obtained as well using the crystallographic data for starting calculations. The obtained data show that independently of the used approximation the obtained data correlated reasonably well with the used conformational analysis.

The FAB mass spectra were recorded on a Fisons VG Autospec instrument employing 3-nitrobenzylalcohol as the matrix.

The elemental analysis was carried out according to the standard procedures for C and H (as CO_2, and H_2O) and N (by the Dumas method).

The thermogravimetric study was carried out using a Perkin-Elmer TGS2 instrument and calorimetry was performed on a DSC-2C Perkin-Elmer apparatus under argon.

^{1}H-NMR measurements, referred to sodium 3-(trimethylsilyl)-tetradeuteropropionate, were performed at 298 K with a Bruker DRX-400 spectrometer using 5 mm tubes and D_2O as solvent.

Results and discussion

Crystal structure

The asymmetric unit of the compound is presented in Fig. 1. A 3D network is formed through hydrogen bonds of the O=C-NH_2 function, the hydrogensquarate ion and the N^+H_3 group, $NH_2\cdots O{=}C_{(Sq)}$ (2.840 and 2.749 Å), $_{(Sq)}OH\cdots O = C(NH_2)$ (2.618 Å), $NH_3{}^+\cdots O{=}C_{(Sq)}$ (3.246, 2.804 and 2.823 Å, respectively (Fig. 2). Like other isolated and structurally characterized ester amides (Kolev et al. 2004, 2005, 2006a, b, c, d, e) of H_2Sq diethyl esters, typical values of bond lengths and angles are observed in this presented case (Table S1). within the cation/anion pair of Fig. 1, the H_2Sq fragment is effectively flat with deviations from the best plane at 0.2(1)° and 0.7(1)°, respectively. The planes of the hydrogensquarate anion and the amide O=C–NH_2 function are near to co-planar (Fig. 2) in the asymmetric unit making an angle of 10.2(4)° (Fig. 2).

Theoretical analysis

Conformational analysis of the compound in the gas phase was performed by energy minimization through optimization of the dihedral angles. Seventeen potential energy minima are predicted for $LeuNH_2{\cdot}HSq$. Only seven are characterized by an E_{rel} lower than 5 kJ/mol (Scheme 3 and Fig. 3), with respect to the most stable conformer C_i of $LeuNH_2{\cdot}HSq$.

The values of the predicted geometry parameters listed in Table S2 (s.m.) correspond to the conformer C_i. The atom numbering scheme is listed in Scheme 1. The

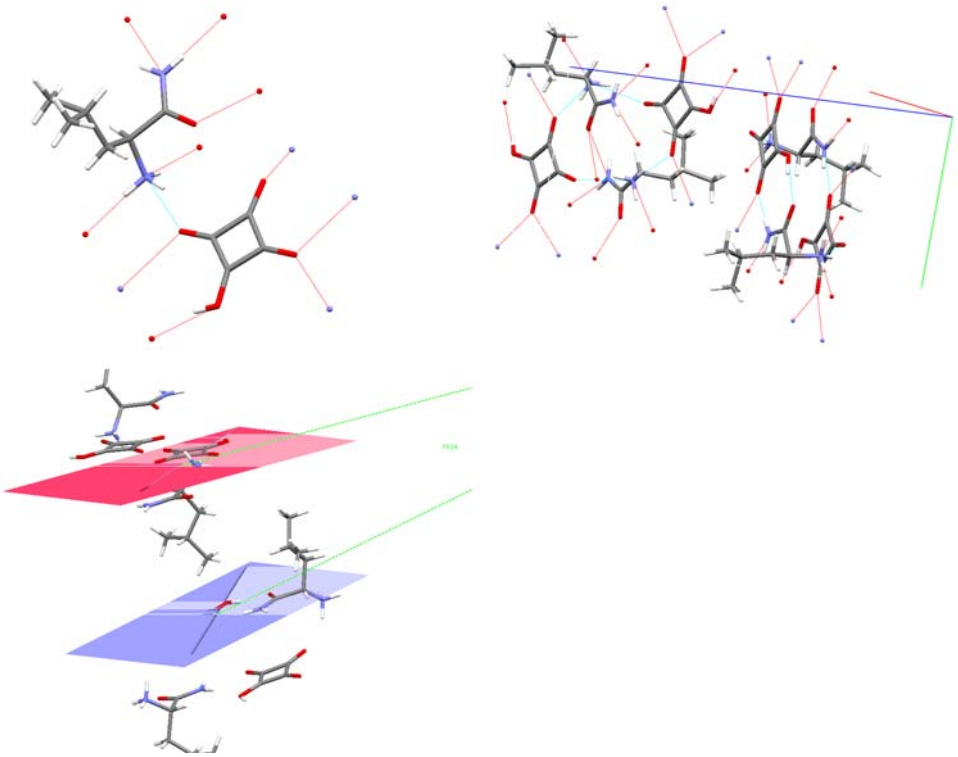

Fig. 2 Hydrogen bonding in the unit cell of the compound. In *red* and *blue* are given the corresponding planes of the squaric acid and amide fragments, included in the unit cell of the compound studied (color in online only)

optimized structural parameters as bond lengths and angles (Table S2) agree reasonably well with those obtained by X-ray diffraction (compared Tables S1 and S2). Comparing the experimental data with the theoretical results, the atomic distances and angles do not differ by more than 0.098 Å, 3.7(5)° and 0.088 Å, 4.8(3)° for hydrogen-squarate and the ester amide of H_2Sq ethyl ester. The obtained data correlated well with the experimental ones for other leucinamide derivatives such as DL-acetyl leucine *N*-methylamide (Ichikawa et al. 1969), *N*-acetyl-L-prolyl-L-leucinamide (Puliti et al. 2001) and phenylalanyl-leucinamide hydrochloride monohydrate (Doi et al. 2003), where the corresponding bond length and angles differences are less than 0.1231 Å, 7.6(6)°, respectively.

A significant deviation is determined on comparing the corresponding data for the dihedral angles in the gas phase and in the solid-state. The calculated values of the D(7, 5, 6, 9) and D(7, 5, 4, 2) dihedral angles of 32.2° and 179.2° are strikingly different to the experimental values of 166.7° and 68.6°, respectively, determined by X-ray structural analysis in protonated $LeuNH_2$. These data may be explained by the presence of strong intermolecular interactions in the solid-state leading to a deviation from the theoretically predicted dihedral angles for the isolated molecule in gas phase (see above and scheme). Similar results have been obtained for di- and tripeptide systems (Kolev et al. 2007b, 2008b). The amide C=O–NH_2 fragment is flat with a maximal deviation from the planarity of 1.0°.

Conventional and linear-polarized IR- spectral data

The experimental confirmation of the assignment of characteristic IR bands is generally achieved by applying preliminary deconvolution and curve-fitting procedures for the determination (Fig. 4a(2) , b(2)) of the peak positions and integral absorbencies. The compound is, however, characterized by a strongly overlapped IR-spectral pattern (Fig. 4a(1) , b(1)). Moreover, the presence of H_2Sq moieties resulted in a series of additional intermolecular interactions which further complicated the IR-spectrum. For these reasons, the adequate interpretation by conventional IR-spectroscopic tools is practically impossible. As a consequence, the experimental confirmation of characteristic IR-band assignments was carried out by IR-LD spectral analysis of the compound in the solid-state, in support of the crystal structure. The data are summarized in Table 2. The application of the reducing-difference procedure leads to the following results. The simultaneous disappearance of the bands at 672 cm^{-1} and 620 cm^{-1} proves their origin as $\omega_{NH2.}$

The elimination of the band at 1,596 cm^{-1} provokes the band at of 3,218 cm^{-1} to vanish, while the reduction of the 1,694 cm^{-1} band leads to disappearance of the bands at 1,575 cm^{-1} and 3,174 cm^{-1}, as a result of co-linearity of the corresponding transition moments in both cases. The participation of the OH group of hydrogen squarate in a strong intermolecular interaction causes the stretching

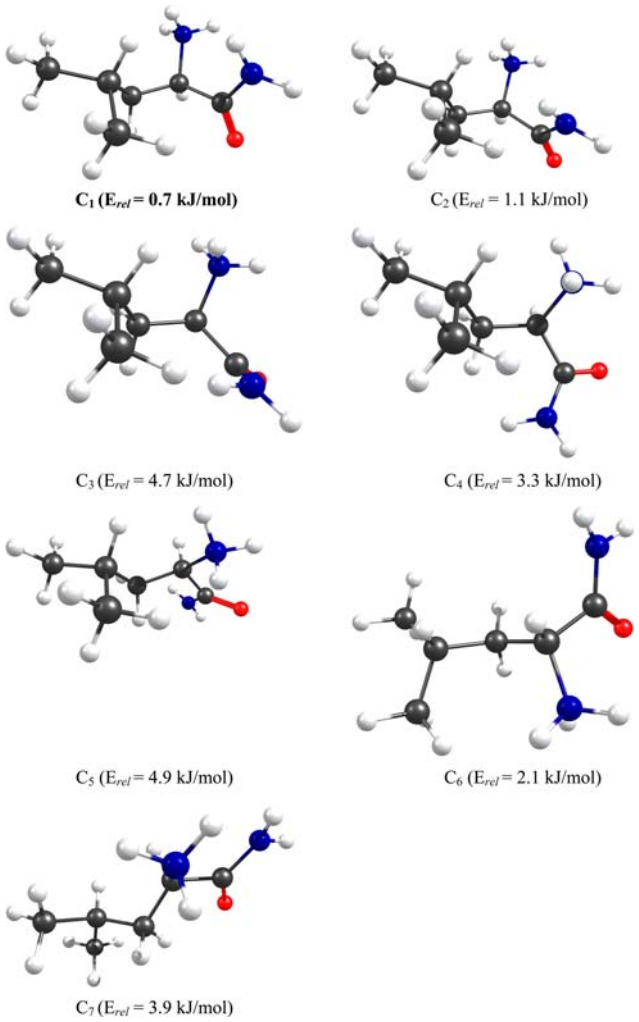

Scheme 3 ab initio conformers of protonated $LeuNH_2$ at the UMP2 level of theory and 6-311++G** basis setwith potential energy minima lower than 5 kJ/mol

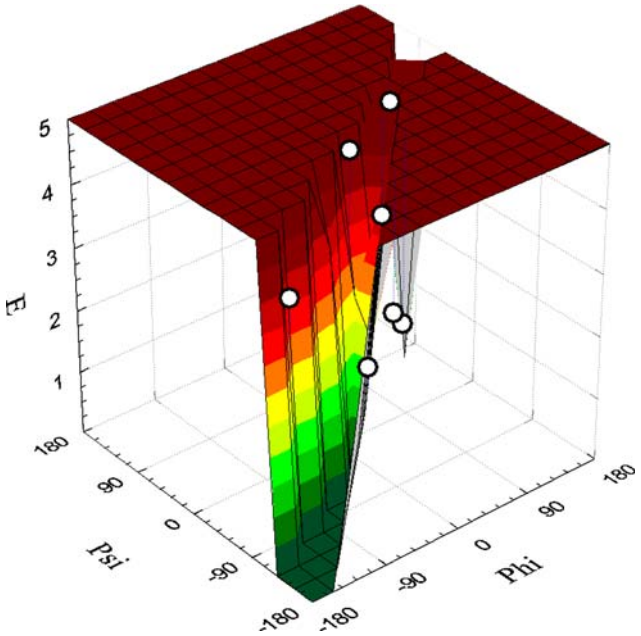

Fig. 3 φ and χ potential energy surface of the protonated $LeuNH_2$. *Dots* denote the obtained stable conformers with the energy values less than 5 kJ/mol. The most stable two of them are observed at Phi values higher than 178.5(1)°

ν_{OH} band to shift to lower frequency at 3,272 cm^{-1} (Fig. 4a(2)).

Conclusion

The structure of the hydrogensquarate of L-leucinamide has been determined by single crystal X-ray diffraction. 3D helix chains are formed through hydrogen bonds with participation of the O=C–NH_2 function, the hydrogensquarate ion and the NH_3 group [$NH_2\cdots O{=}C_{(Sq)}$ (2.840 and 2.749 Å), $_{(Sq)}OH\cdots O{=}C(NH_2)$ (2.618 Å), $NH_3^+\cdots O{=}C(Sq)$ (3.246, 2.804 and 2.823 Å)], respectively. The UMP2 and MP2 level of theory at the 6-311++G** basis have been employed to calculate the geometries of most stable conformers in the gas phase. The IR-spectroscopic assignment in solid-phase has been obtained by linear-polarized IR-spectroscopy of oriented samples as suspensions in a nematic liquid crystal and application of the reducing-difference procedure for polarized IR-spectra interpretation. A deconvolution and curve-fitting procedure was applied in parallel to the spectral pattern. The compound was characterized by ^{1}H-NMR data in solution. The series of investigations on our group on the conformational preference in solid-state of the amino acids and their derivatives show that the usage of the H_2Sq as corresponding counter ion in the crystals of these systems is fruitful tool for analysis of the correlation structure-spectroscopic properties. A considerable progress in recent years by controlling the assembly of individual molecules in solids is obtained. By tuning the hydrogen bonding as a powerful non-covalent force for organizing organic molecules a series of derivatives of H_2Sq with small biologically active compound have been obtained (Ivanova et al. 2004, 2006, 2007; Koleva et al. 2008). H_2Sq provides an attractive template for generating tightly hydrogen bonded self-assemblies from polarizable cations in general and basic amino acids in particular. The self-assembly patterns of H_2Sq itself and its anions HSq^- and Sq^{2-} have been identified. It is reasonable to expect that a further systematic variation of the counterion in salts of the HSq^- and/or Sq^{2-} anions should lead to the isolation of additional different conformers of the amino acids and their derivatives, diving a possibility for direct elucidation of the relationship structure-spectroscopic properties of these systems. More over it is found that the H_2Sq derivatives of the amino acid amides and small peptides allow the crystallization of different conformers of the cations, depending of the included solvent molecules

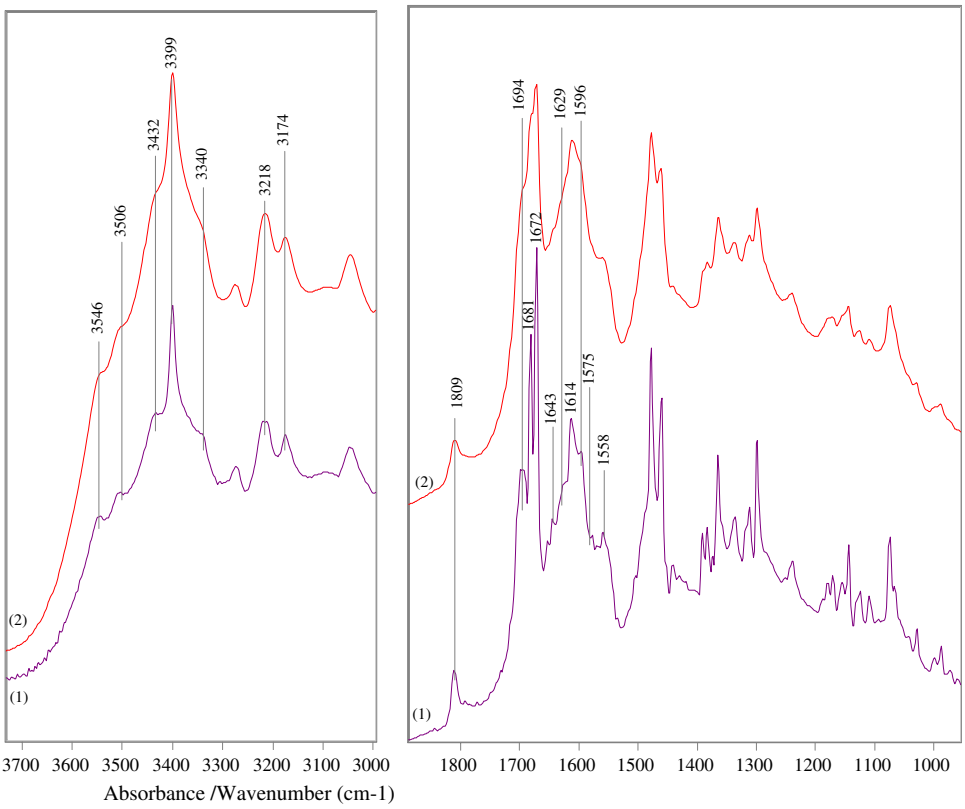

Fig. 4 Deconvoluted and non-affected solid-state IR-spectra of $LeuNH_2$·HSq

Table 2 IR-characteristic frequencies of $LeuNH_2$·HSq in the solid-state

ν (cm^{-1})	Assignment	ν (cm^{-1})	Assignment
3,399, 3,218	$\nu^{as}_{NH_2}$, $\nu^{s}_{NH_2}$	1175	$\delta_{CH} + \nu_{CN} + \nu_{CC}$
3,272	$\nu_{OH(Sq)}$	1075	ρ_{NH2}
1,809	$\nu^{s}_{C=O\ (Sq)}$	713	τ_{NH2}
1,672	$\nu^{as}_{C=O\ (Sq)}$	672	$\omega_{NH2} + \delta_{CO}$
1,681	$\nu_{C=O\ (Amide\ I)}$	620	$\delta_{CO} + \omega_{NH_2}$
1,614	$\nu_{C=C\ (Sq)}$	433	$\gamma_{C=O(Sq)}$
1,596	δ_{NH_2}(Amide II)		
1,363	$\nu_{CN(Amide)} + \nu_{CC}$		

as well. In this respect the structural elucidation of series of amino acid derivatives of amino acids and H_2Sq depending of the included solvents in the unit cell, are now in progress.

Acknowledgments B. B. K. wishes to thank the Alexander von Humboldt Foundation for the Fellowship and T.K. the DAAD for a grant within the priority program "Stability Pact South-Eastern Europe" and the Alexander von Humboldt Foundation. Supporting information: Crystallographic data for the structural analysis have been deposited with the Cambridge Crystallographic Data Centre, CCDC 693631 Copies of this information may be obtained from the Director, CCDC, 12 Union Road, Cambridge, CB2 1EZ, UK (Fax: +44 1223 336 033; e-mail: deposit@ccdc.cam.ac.uk or http://www.ccdc.cam.ac.uk).

References

Chemla D, Zyss J (eds) (1987) Nonlinear optical properties of organic molecules and crystals, vol 1. Academic Press, New York, pp 23–187

Doi M, Asano A, Yamamoto D (2003) Hydrogen bond between water and the phenyl ring in the structure of a dipeptide H–Phe–Leu–NH_2 at 90 K and the structure-based energy estimations. Chem Lett 32:1102–1003

Eipper BA, Mains RE (1988) Peptide alpha-amidation. Annu Rev Physiol 50:333–344. doi:10.1146/annurev.ph.50.030188.002001

Head-Gordon H, Head-Gordon M, Frisch MJ, Brooks CIII, Pople J (1991) Theoretical study of blocked glycine and alanine peptide analogs. J Am Chem Soc 113:5989–5997. doi:10.1021/ja00016a010

Ichikawa T, Iitaka Y (1969) The crystal structure of DL-acetylleucine *N*-methylamide, $C_9H_{18}O_2N_2$. Acta Crystallogr 25B:1824–1833

In Y, Fujii M, Sasada Y, Ishida Y (2001) Structural studies on C-amidated amino acids and peptides: structures of hydrochloride salts of C-amidated Ile, Val, Thr, Ser, Met, Trp, Gln and Arg, and comparison with their C-unamidated counterparts. Acta Crystallogr B 57:72–81. doi:10.1107/S0108768100013975

Ivanova BB, Arnaudov MG, Bontchev PR (2004) IR/LD analysis of Cu(I) complex of homocysteine. Spectrochim Acta 60A:855

Ivanova BB, Tsalev DL, Arnaudov MG (2006) Validation of reducing-difference procedure for the interpretation of non-polarized infrared spectra of n-component solid mixtures. Talanta 69:822–828. doi:10.1016/j.talanta.2005.11.026

Ivanova BB, Simeonov V, Arnaudov M, Tsalev D (2007) Linear-dichroic infrared spectroscopy—validation and experimental design of the orientation technique as suspension in nematic liquid crystal. Spectrochim Acta [A] 67A:66–75. doi:10.1016/j.saa.2006.06.025

Kim CU, Misco PF (1992) A facile synthesis of 1-Hydroxy-2-phosphonocyclobutenedione. Tetrahedron Lett 33:3961–3962. doi:10.1016/0040-4039(92)88072-D

Kolev T, Petrova R, Spiteller M (2004) (*R*)-2-[(2-Ethoxy-3, 4-dioxocyclobut-1-en-1-yl)amino]-3-phenylpropanamide hemihydrate. Acta Crystallogr E 60:o634

Kolev T, Spiteller M, Sheldrick WS, Mayer-Figge H (2005) 1-(Aminocarbonyl)ethylammonium hydrogensquarate monohydrate. Acta Crystallogr E 61:o4292–o4293

Kolev T, Spiteller M, Sheldrick WS, Mayer-Figge H, Van Almsick T (2006a) L-Tyrosinamide hydrochloride monohydrate. Acta Crystallogr E 61:o3819

Kolev T, Cherneva E, Spiteller M, Sheldrick WS, Mayer-Figge H (2006b) L-Methioninamide ester amide of squaric acid diethyl ester. Acta Crystallogr E 62:o1390–o1392

Kolev T, Koleva BB, Cherneva E, Spiteller M, Sheldrick WS, Mayer-Figge H (2006c) Crystal structure, IR-LD spectroscopic, theoretical and vibrational analysis of valinamide ester amide of squaric acid diethyl ester. Struct Chem 17:491–499. doi:10.1007/s11224-006-9071-8

Kolev T, Yancheva D, Spiteller M, Sheldrick WS, Mayer-Figge H (2006d) L-Prolinamidium hydrogensquarate. Acta Crystallogr E 62:o463–o464

Kolev T, Spiteller M, Sheldrick WS, Mayer-Figge H (2006e) L-Argininamidium bis(hydrogensquarate). Acta Crystallogr C 62:o299–o300. doi:10.1107/S0108270106012108

Kolev T, Koleva BB, Spiteller M (2007a) Spectroscopic and theoretical characterization of hydrogensquarates of L-threonyl-L-serine and L-serine prediction of structures of the neutral and protonated forms of the dipeptide. Amino Acids 33:719–725. doi:10.1007/s00726-006-0391-1

Kolev T, Koleva BB, Seidel RW, Mayer-Figge H, Spiteller M, Sheldrick WS (2007b) Tyrammonium 4-nitrophthalate dihydrate—structural and spectroscopic elucidation. Amino Acids. doi:10.1007/s00726-007-0021-6

Kolev TM, Koleva BB, Spiteller M, Sheldrick WS, Mayer-Figge H (2008a) Synthesis, spectroscopic and structural elucidation of tyrosinamide hydrogensquarate monohydrate. Amino Acids. doi:10.1007/s00726-008-0047-4

Kolev TM, Koleva BB, Spiteller M, Sheldrick WS, Mayer-Figge H (2008b) Synthesis, spectroscopic and structural elucidation of sympathomimetic amine, tyraminium dihydrogenphosphate. Amino Acids. doi:10.1007/s00726-008-0046-5

Koleva BB, Kolev TM, Simeonov V, Spassov T, Spiteller M (2008) Linear polarized IR-spectroscopy of partial oriented solids as a colloid suspension in nematic liquid crystal—new tool for structural elucidation of the chemical compounds. J Inclus Prenome. doi:10.1007/s10847-008-9425-5

Kulathila R, Merkler KA, Merkler DJ (1999) Enzymatic formation of C-terminal amides. Nat Prod Rep 16:145–155. doi:10.1039/a801346b

Merkler D (1994) C-Terminal amidated peptides: production by the in vitro enzymatic amidation of glycine-extended peptides and the importance of the amide to bioactivity. J Enzyme Microb Technol 16:450–456. doi:10.1016/0141-0229(94)90014-0

Michl J, Thulstrup E (1986) Spectroscopy with polarized light. Solute alignment by photoselection, in liquid crystals, polymers, and membranes. VCH Publishers, New York

Nalwa HS, Watanabe T, Miyata S (1997) In: Nalwa HS, Miyata S (eds) Nonlinear optics of organic molecules and polymers. CRC Press, Boca Raton, pp 89–29

Gaussian 98: Frisch MJ, Trucks GW, Schlegel HB, Scuseria GE, Robb MA, Cheeseman JR, Zakrzewski VG, Montgomery Jr JA, Stratmann R, Burant C, Dapprich S, Millam M, Daniels A, Kudin K, Strain M, Farkas P, Tomasi J, Barone V, Cossi M, Cammi R, Mennucci B, Pomelli C, Adamo C, Clifford S, Ochterski J, Petersson GA, Ayala PY, Cui Q, Morokuma K, Salvador P, Dannenberg JJ, Malick DK, Rabuck AD, Raghavachari K, Foresman JB, Cioslowski J, Ortiz JV, Baboul AG, Stefanov BB, Liu G, Liashenko A, Piskorz P, Komáromi I, Gomperts R, Martin RL, Fox DJ, Keith T, Al-Laham MA, Peng CY, Nanayakkara A, Challacombe M, Gill PMW, Johnson B, Chen W, Wong MW, Andres JL, Gonzalez C, Head-Gordon M, Replogle ES, Pople JP. *Gaussian 98*. Gaussian, Inc., Pittsburgh, 1998

Puliti R, Mattia CA, Giancola C, Barone G (2001) Crystal structure and conformational stability of *N*-acetyl-L-prolyl-L-leucinamide. Comparison between structural and thermophysical data. J Mol Struct 553:117–130. doi:10.1016/S0022-2860(00)00537-8

Ramachandran G, Sasisekharan V (1968) Conformation of polypeptides and proteins. Adv Protein Chem (Kyoto) 23:283–437

Sheldrick GM (1997a) SHELXS-97. Program for crystal structure solution. University of Cottingen, Germany

Sheldrick GM (1997b) SHELXL-97. Program for crystal structure solution. University of Cottingen, Germany

Suwan S, Isobe M, Yamashita O, Minakata H, Imai K (1994) Silkworm diapause hormone, structure–activity relationships indispensable role of C-terminal amide Ins Biochem. Mol Biol 24:1001–1007

Sztaricskai F, Sum A, Roth E, Pelyvas I, Sandor S, Batta G, Herczegh P, Remenyi P, Miklan Z, Hudecz F (2005) A new class of semisynthetic anthracycline glycoside antibiotics incorporating a squaric acid moiety. J Antibiot 58:704–714

Tevyashova A, Sztaricskai F, Batta G, Herczegh P, Jeney A (2004) Formation of squaric acid amides of anthracycline antibiotics synthesis and cytotoxic properties. Bioorg Med Chem Lett 14:4783–4789. doi:10.1016/j.bmcl.2004.06.072

Vargas R, Garza J, Hay B, Dixon D (2002) Conformational study of the alanine dipeptide at the MP2 and DFT levels. J Phys Chem A 106:3213–3218. doi:10.1021/jp013952f

Wolff JJ, Wortmann R (1999) For a general introduction to non-linear optics of organic compounds. Adv Phys Org Chem 32:121–152. doi:10.1016/S0065-3160(08)60007-6

Xie J, Comeau AB, Seto CT (2004) Squaric Acids: a new motif for designing inhibitors of protein tyrosine phosphatases. Org Lett 6:83–86. doi:10.1021/ol036121w

Zimmerman S, Pottle M, Nemethy G, Scheraga H (1977) Conformational analysis of the 20 naturally occurring amino acid residues using ECEPP. Macromolecules 10:1–9